

# A novel human R25C-phospholamban mutation is associated with super-inhibition of calcium cycling and ventricular arrhythmia

Guan-Sheng Liu<sup>1</sup>, Ana Morales<sup>2,3</sup>, Elizabeth Vafiadaki<sup>4</sup>, Chi Keung Lam<sup>1</sup>, Wen-Feng Cai<sup>5</sup>, Kobra Haghighi<sup>1</sup>, George Adly<sup>1</sup>, Ray E. Hershberger<sup>2,3,6</sup>, and Evangelia G. Kranias<sup>1,4\*</sup>

<sup>1</sup>Department of Pharmacology and Cell Biophysics, University of Cincinnati College of Medicine, PO Box 670575, 231 Albert Sabin Way, Cincinnati, OH, USA; <sup>2</sup>Division of Human Genetics, Ohio State University College of Medicine, Columbus, OH, USA; <sup>3</sup>Dorothy M. Davis Heart and Lung Research Institute, Ohio State University College of Medicine, Columbus, OH 45267-0575, USA; <sup>4</sup>Molecular Biology Division, Biomedical Research Foundation, Academy of Athens, Greece; <sup>5</sup>Department of Pathology and Laboratory Medicine, University of Cincinnati College of Medicine, Cincinnati, OH, USA; and <sup>6</sup>Division of Cardiovascular Medicine, Department of Internal Medicine, Ohio State University College of Medicine, Columbus, OH, USA

Received 11 December 2014; revised 2 March 2015; accepted 20 March 2015; online publish-ahead-of-print 7 April 2015

Time for primary review: 28 days

**Aims** Depressed sarcoplasmic reticulum (SR) Ca<sup>2+</sup> cycling, a universal characteristic of human and experimental heart failure, may be associated with genetic alterations in key Ca<sup>2+</sup>-handling proteins. In this study, we identified a novel PLN mutation (R25C) in dilated cardiomyopathy (DCM) and investigated its functional significance in cardiomyocyte Ca<sup>2+</sup>-handling and contractility.

**Methods and results** Exome sequencing identified a C73T substitution in the coding region of *PLN* in a family with DCM. The four heterozygous family members had implantable cardiac defibrillators, and three developed prominent ventricular arrhythmias. Overexpression of R25C-PLN in adult rat cardiomyocytes significantly suppressed the Ca<sup>2+</sup> affinity of SR Ca<sup>2+</sup>-ATPase (SERCA2a), resulting in decreased SR Ca<sup>2+</sup> content, Ca<sup>2+</sup> transients, and impaired contractile function, compared with WT-PLN. These inhibitory effects were associated with enhanced interaction of R25C-PLN with SERCA2, which was prevented by PKA phosphorylation. Accordingly, isoproterenol stimulation relieved the depressive effects of R25C-PLN in cardiomyocytes. However, R25C-PLN also elicited increases in the frequency of Ca<sup>2+</sup> sparks and waves as well as stress-induced aftercontractions. This was accompanied by increased Ca<sup>2+</sup>/calmodulin-dependent protein kinase II activity and hyper-phosphorylation of RyR2 at serine 2814.

**Conclusion** The findings demonstrate that human R25C-PLN is associated with super-inhibition of SERCA2a and Ca<sup>2+</sup> transport as well as increased SR Ca<sup>2+</sup> leak, promoting arrhythmogenesis under stress conditions. This is the first mechanistic evidence that increased PLN inhibition may impact both SR Ca<sup>2+</sup> uptake and Ca<sup>2+</sup> release activities and suggests that the human R25C-PLN may be a prognostic factor for increased ventricular arrhythmia risk in DCM carriers.

**Keywords** Dilated cardiomyopathy • Calcium cycling • Mutation

## 1. Introduction

Dilated cardiomyopathy (DCM), a common cause of heart failure, is characterized by dilation and impaired contraction of the left ventricle. Multiple aetiologies may underlie DCM, including rare variants in more than 30 genes, which initiate diverse pathophysiological mechanisms leading to left-ventricular dysfunction or arrhythmia and increased morbidity and mortality.<sup>1</sup>

A common clinical hallmark and characteristic of failing cardiomyocytes is the defective Ca<sup>2+</sup> homeostasis, exhibited by a prolonged

decay time of intracellular Ca<sup>2+</sup> transient and changes in systolic and diastolic Ca<sup>2+</sup> levels.<sup>2–4</sup> The prolonged Ca<sup>2+</sup>-transient decay time and increased diastolic Ca<sup>2+</sup> levels may result from impaired ryanodine receptor function, decreased sarcoplasmic reticulum Ca<sup>2+</sup>-ATPase (SERCA2a) levels, and augmented SERCA2a inhibition by phospholamban (PLN).<sup>5</sup> PLN is a prominent regulator of Ca<sup>2+</sup> cycling and a primary mediator of the  $\beta$ -adrenergic effects resulting in enhanced cardiac output.<sup>6,7</sup> In the dephosphorylated state, PLN inhibits SERCA2a and shifts its Ca<sup>2+</sup> activation towards lower apparent Ca<sup>2+</sup> affinity. However, upon PKA-mediated phosphorylation, the inhibition on SERCA2a by PLN is relieved

\* Corresponding author. Tel: +513 558 2377; fax: +513 558 0646, Email: litsa.kranias@uc.edu

and its  $\text{Ca}^{2+}$  affinity is increased.<sup>7</sup> Thus, PLN plays a key role in the regulation of  $\text{Ca}^{2+}$  reuptake by SERCA2a to induce relaxation and decrease diastolic  $\text{Ca}^{2+}$  levels. It is also a prominent mediator of the  $\beta$ -adrenergic stimulatory responses in the heart.<sup>7</sup>

The important role of PLN in cardiac function has prompted searches for human PLN genetic variants, which may be associated with DCM. Indeed, four mutations have been identified in the coding region of *PLN*. The first mutation was V49G, which resulted in potent inhibition of the  $\text{Ca}^{2+}$  affinity of SERCA2a. Cardiac overexpression of the V49G mutant PLN in mouse led to super-inhibition of cardiac contractility and remodelling, which progressed to DCM and early mortality.<sup>8</sup> The second mutation identified had a stop codon for Leucine 39 (L39X-PLN) with onset of DCM and heart failure during the teenage years.<sup>9</sup> The third human mutation, R9C, had no effects on SERCA2a activity under basal conditions but appeared to trap PKA, which blocked PKA-mediated phosphorylation of even wild-type PLN. The detrimental effects of such chronic inhibition of SERCA2a activity resulted in DCM.<sup>10</sup> The fourth PLN mutation was a deletion of Arg-14 (Arg14Del).<sup>11</sup> It was found that heterozygous carriers exhibited inherited DCM with left-ventricular dilation, contractile dysfunction, variable conduction system disease with episodes of malignant ventricular arrhythmias in some carriers and death by middle age.<sup>12,13</sup> The mechanism underlying the detrimental effects of this human mutation involves super-inhibition of SERCA2a activity, likely mediated through a disturbance in the structure of PLN.<sup>11</sup> These findings add to accumulating evidence that myocellular calcium dysregulation caused by mutations in human *PLN* is sufficiently deleterious to cause DCM and initiate heart failure.

In this study, we report a new mutation (R25C) in the coding region of the human *PLN* gene (*PLN*), identified in a pedigree with DCM that also showed prominent ventricular arrhythmia and need for implantable cardiac defibrillators (ICDs).<sup>14,15</sup> Exome sequencing of affected family revealed that they had a R25C-PLN mutation, which was associated with super-inhibition of SERCA2a, depressed myocyte contractile and  $\text{Ca}^{2+}$ -kinetic parameters and increased arrhythmias in cardiomyocytes. The mechanisms underlying the detrimental effects of this mutation include enhanced interaction of R25C-PLN mutant with SERCA2a, leading to super-inhibition of SERCA2a activity and increased Cam kinase II (CaMKII) activity associated with hyper-phosphorylation of Serine 2814 in RyR.

## 2. Methods

For details regarding methods, refer to the Supplementary material online, Methods.

### 2.1 Identification of a PLN mutation and generation of adenoviruses

For the human study, written informed consent was obtained and methods were conducted in accordance with the Declaration of Helsinki, and the study was approved by the Institutional Review Boards of Oregon Health and Science University and the University of Miami in FL, USA. Genomic DNA was extracted using standard procedures and *PLN* exomes were sequenced.<sup>15,16</sup> Adenoviruses expressing green fluorescent protein (Ad.GFP), WT-PLN (Ad.WT), and R25C-PLN (Ad.R25C) were generated.<sup>9</sup>

### 2.2 Myocyte culture and quantitative immunoblotting

Animals were handled according to the Institutional Animal Care and Use Committee at the University of Cincinnati. Myocytes from adult male rats were isolated,<sup>17</sup> cultured for 2 h and infected with adenoviruses. At 24 h

post-infection, we determined PLN levels by western blots and initial rates of SR  $\text{Ca}^{2+}$  uptake.<sup>18</sup> Data were analysed by non-linear regression using the OriginLab 5.1 program.

### 2.3 Cardiomyocyte contractility and $\text{Ca}^{2+}$ transients

Contractions were obtained at 0.5 Hz and  $\text{Ca}^{2+}$  kinetics were determined in cells loaded with Fura-2 /AM and excited at 340 and 380 nm.

### 2.4 HEK 293 cells, immunofluorescence, and immunoprecipitation

HEK 293 cells were transfected with GFP-PLN and SERCA2 constructs,<sup>19</sup> fixed, blocked, and incubated with SERCA2 antibody. Samples were counterstained with Alexa Fluor anti-mouse 568 secondary antibody, mounted with Vectashield medium containing DAPI and analysed by confocal microscopy. In parallel, transfected HEK 293 cells were lysed and processed for immunoprecipitation.

### 2.5 Measurement of $\text{Ca}^{2+}$ sparks, waves, and diastolic SR $\text{Ca}^{2+}$ leak

Spontaneous  $\text{Ca}^{2+}$  sparks and waves were obtained in quiescent cells loaded with Rhod-2 AM. Diastolic SR  $\text{Ca}^{2+}$  leak was measured using the tetracaine method.<sup>20</sup>

### 2.6 Aftercontractions in rat cardiomyocytes

Rat ventricular myocytes were paced at 2 Hz in the presence of 1  $\mu\text{mol/L}$  ISO. After 2 or 3 trains of stimulation, pacing was stopped and spontaneous aftercontractions within 2–5 s were recorded.

### 2.7 CaMKII activity assay

Cell lysates from infected myocytes were processed for CaMKII activity (Cyclax Kit, MBL International, Woburn, MA, USA).

### 2.8 Statistics

Results are expressed as mean  $\pm$  SEM. Comparisons were evaluated by one-way ANOVA and a *post-hoc* Tukey test. Fisher's exact test was used for calcium sparks, waves, and after contractions. Values of  $P < 0.05$  were considered significant.

## 3. Results

### 3.1 Identification of a novel PLN mutation in a familial DCM pedigree

Forty-eight variants, meeting our established criteria for exome sequencing analysis,<sup>15</sup> were identified in two sisters (III.1 and III.3) in our family pedigree (Figure 1). Of these 48, three were in previously identified DCM genes, including a novel heterozygous *PLN* mutation that resulted in change of arginine into cysteine at position 25, and two missense mutations in *Titin* (*TTN*) (A3656S and P7178S). Because it is known that even rare (<0.5%) *TTN* missense mutations are prevalent in control samples,<sup>16,21</sup> these missense variants were considered unlikely to be the cause of DCM. The *PLN* mutation had high conservation scores (Phastcons 1; GERP 4.31), and based on other heterozygous *PLN* missense mutations causing DCM,<sup>8–11</sup> it was hypothesized that this mutation also may alter *PLN* activity. None of the genes harbouring the remaining 45 variants were associated with known cardiovascular disorders. No additional *PLN* variants were identified in 16 other families.<sup>15</sup>

A pedigree with the *PLN* mutation status is shown in Figure 1. Sanger sequencing confirmed that the *PLN* mutation was present in the sisters (III.1 and III.3), the proband (III.2) who also carried a previously

identified *LMNA* mutation,<sup>15</sup> as well as in his mother (II.3), who had DCM but was not found to carry the *LMNA* mutation.<sup>15</sup>

### 3.2 Clinical characteristics

Clinical characteristics of family members with the *PLN* mutation are provided (Table 1). The proband (III.2) presented at age 47 with sudden cardiac arrest and was diagnosed with non-ischaemic DCM upon resuscitation. An ICD was placed from which he has received multiple appropriate shocks. Approximately 10 years later, he required heart transplantation due to worsening heart failure. Two of his sisters were also found to harbour the R25C-*PLN* mutation. His older sister (III.1) was first screened clinically at age 51 and was found to have left-ventricular enlargement but preserved systolic function. Despite already receiving an angiotensin receptor blocker (ARB), 2 years later her ventricular function had deteriorated. Non-sustained ventricular tachycardia (NSVT) was found on Holter monitoring, and an ICD was placed prior to the onset of any heart failure. She was treated with full-dose beta blockade and an ARB. Over the course of the following 10 years, two cardioversions were required due to persistent atrial fibrillation. The proband's younger sister (III.3), who also had NSVT and

required an ICD, was diagnosed with DCM at age 45 after presenting with signs of heart failure. Their mother (II.3), who had complained of palpitations since age 47, had premature ventricular contractions at age 57. She was diagnosed with DCM at 71 and had multiple PVCs, couplets, and NSVT for years, for which an ICD was placed at age 84 because of progressive pump dysfunction. She progressed to chronic atrial fibrillation and received multiple cardioversions, and died from heart failure at age 90.

### 3.3 Expression of mutant *PLN* in adult cardiomyocytes and $Ca^{2+}$ uptake assay

To determine whether the inhibitory effects of *PLN* on cardiac contractility are modified by the R25C mutation, recombinant adenoviruses encoding GFP, WT-*PLN*, or R25C-*PLN* were transduced into adult rat ventricular myocytes. The protein levels of *PLN* in infected cardiomyocytes were assessed by SDS-PAGE and western blots. Quantitative immunoblotting of cell lysates revealed a similar ratio of *PLN* pentamers to monomers in mutant *PLN* (85.8%) cardiomyocytes, compared with WT-*PLN* (86.6%) and GFP (84.9%) groups (Figure 2A). Furthermore, upon boiling the cardiac homogenates prior to SDS-PAGE, the

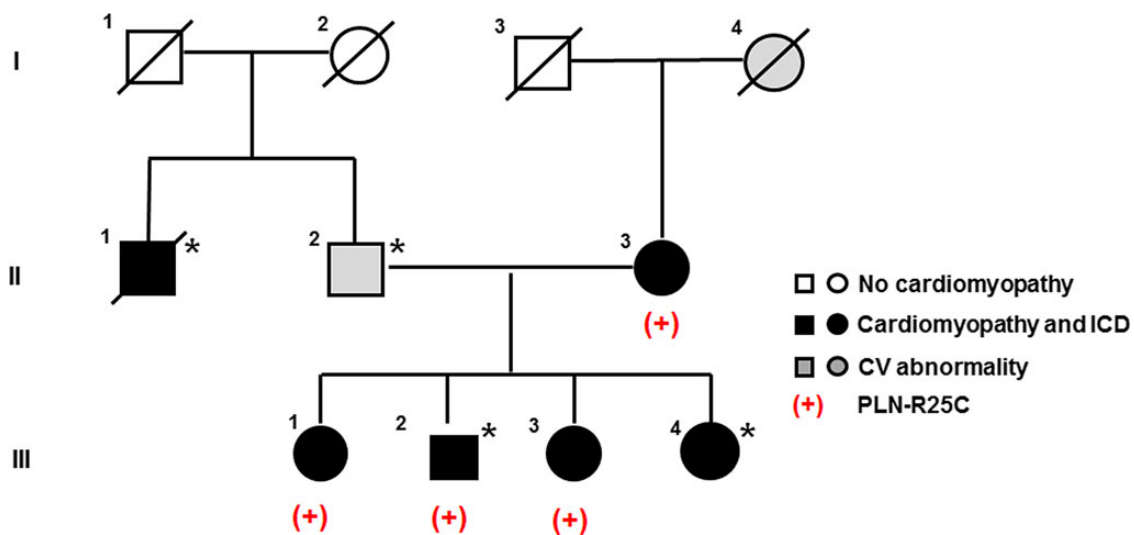


**Figure 1** Familial DCM Pedigree with a *PLN* mutation. Squares represent males and circles represent females. Slash denotes deceased. Darkened symbols indicate idiopathic DCM with implantable cardiac defibrillator (ICD) and grey symbols represent a significant cardiovascular abnormality. Open symbols represent negative cardiovascular history. The presence of the *PLN* mutation is denoted with (+) and the presence of the *LMNA* mutation<sup>14</sup> with asterisk.

**Table 1** Clinical characteristics of family members with the R25C-*PLN* mutation

Pedigree position	DCM	Age of diagnosis, years	LVEDD, mm (Z-score)	LVEF, %	ECG/Arrhythmia	Comment
II.3	Yes	71	60 (4.1)	35	AF, PVCs, LBBB, ICD	HF
III.1	Yes	53	58 (3.4)	40	AF, 1AVB, VT, ICD	HF
III.2	Yes	47	72 (4.85)	28	AF, RBBB, PM/ICD VT, SCD	Heart transplant at 58 years
III.3	Yes	45	59.6 (3.99)	17	NSVT, PM/ICD	HF

LVEDD, left-ventricular end-diastolic dimension by echocardiography; Z-score, number of standard deviations of the LVEDD above the population mean; EF, left-ventricular ejection fraction; AF, atrial fibrillation; PVCs, premature ventricular contractions; LBBB, left bundle branch block; ICD, implantable cardiac defibrillator; HF, heart failure; 1AVB, first-degree atrioventricular block; VT, ventricular tachycardia; RBBB, right bundle branch block; PM, pacemaker; SCD, sudden cardiac death; NSVT, non-sustained ventricular tachycardia.

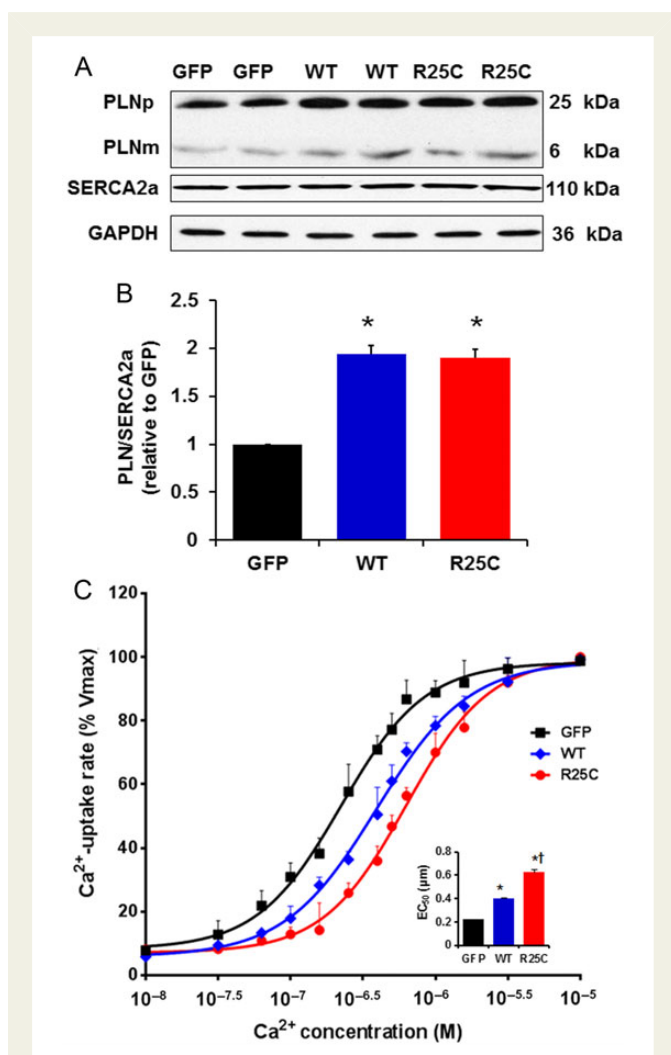


**Figure 2** Quantitative immunoblots from infected cardiomyocytes and Ca<sup>2+</sup> uptake assays. (A) Representative blots of PLN and SERCA. PLNp, pentameric PLN; PLNm, monomeric PLN; (B) PLN protein levels in GFP, WT and R25C cardiomyocytes expressed as relative ratio of PLN/SERCA2a ( $n = 4$  hearts); (C) Effects of wild-type and mutant R25C-PLN on the apparent Ca<sup>2+</sup> affinity of SERCA2a. After 24-h infection with adenoviruses, cardiomyocytes were homogenized and the initial rates of oxalate-supported SR Ca<sup>2+</sup> uptake were measured. Data are expressed as per cent of maximal uptake rates in each group ( $V_{max}$ :  $99 \pm 4$  in GFP,  $101 \pm 3$  in WT, and  $96 \pm 5$  in R25C, nmol/mg/min). Inset: The average EC<sub>50</sub> values for the three groups ( $n = 6$  hearts). \* $P < 0.05$ , vs. GFP; † $P < 0.05$ , vs. WT. Values are mean  $\pm$  SE.

mutant could be dissociated into monomers, similar to WT-PLN. There were no significant changes in the SERCA2a protein levels in the infected mutant cardiomyocytes (Figure 2A). When the apparent PLN/SERCA2a ratio was calculated, it was found to be a 1.9-fold in R25C myocytes, compared with the GFP group, and this ratio was similar to that for WT-PLN (1.93) (Figure 2B).

To examine the functional significance of the R25C substitution in PLN and its impact on SERCA2a regulation, the initial rates of ATP-dependent, oxalate-facilitated SR Ca<sup>2+</sup> uptake were measured in cell lysates from infected cardiomyocytes. There were no significant differences in the maximal rates of SR Ca<sup>2+</sup> uptake between GFP, WT, or

R25C groups. However, the EC<sub>50</sub> value for Ca<sup>2+</sup> dependence of Ca<sup>2+</sup> uptake was significantly higher in WT-PLN cells ( $0.40 \pm 0.03 \mu\text{M}$ ), compared with the GFP group ( $0.22 \pm 0.02 \mu\text{M}$ ), consistent with our previous findings.<sup>22</sup> Interestingly, R25C-PLN further increased the SERCA2a EC<sub>50</sub> value to  $0.63 \pm 0.07 \mu\text{M}$  (Figure 2C). Thus, the mutant PLN is a super-inhibitor of the affinity of SERCA2a for Ca<sup>2+</sup> compared with WT-PLN.

### 3.4 Functional analysis of the R25C-PLN mutant

Overexpression of WT-PLN has been shown to lead to significant depression of cardiomyocyte function.<sup>22</sup> To determine whether the super-inhibitory effects of the R25C mutation on SERCA2a activity translated into alterations at the cellular level, the contractile parameters of infected cardiomyocytes were assessed. The resting cell length in mutant PLN infected myocytes was not altered compared with the WT-PLN or GFP groups. However, the amplitude of basal cell contraction (fractional shortening, FS%) was more depressed in myocytes overexpressing R25C mutant PLN (60%) than in myocytes overexpressing WT-PLN (76%), compared with GFP control (100%) (Figure 3A and B). The maximal velocities of cardiomyocyte shortening and re-lengthening were also more depressed in myocytes with mutant PLN (+dL/dt: 52%; -dL/dt: 46%) than in cells with WT-PLN (+dL/dt: 67%; -dL/dt: 66%), compared with GFP controls (100%) (Figure 3C and D).

### 3.5 Overexpression of R25C-PLN significantly suppresses Ca<sup>2+</sup> transients, delays the rate of Ca<sup>2+</sup> removal, and elevates intracellular diastolic Ca<sup>2+</sup>

To determine whether the observed alterations in myocyte mechanics reflected similar alterations in Ca<sup>2+</sup> handling, intracellular Ca<sup>2+</sup> transients in infected cardiomyocytes were measured by use of the Fura-2/AM fluorescence indicator (2  $\mu\text{M}$ ). Our results demonstrate that the amplitude of Ca<sup>2+</sup> transients was reduced by 55% in mutant-PLN and by 37% in WT-PLN, compared with GFP cardiomyocytes (Figure 4A and B). The time to 50% decay of the Ca<sup>2+</sup> signal was prolonged by 65% in cardiomyocytes overexpressing mutant and by 32% in cardiomyocytes overexpressing WT-PLN, relative to GFP group (Figure 4C). In addition, intracellular diastolic Ca<sup>2+</sup> was also analysed and it was found to be increased by 18% in R25C-PLN compared with WT-PLN or GFP cardiomyocytes (Figure 4D). Thus, the R25C-PLN mutant depressed mechanical and Ca<sup>2+</sup> kinetic parameters and increased diastolic Ca<sup>2+</sup> levels, consistent with the enhanced inhibition of SERCA2a.

The effects of mutant-PLN on intracellular Ca<sup>2+</sup> transients prompted further studies on the influence of R25C-PLN on SR Ca<sup>2+</sup> load. It was observed that the caffeine-induced Ca<sup>2+</sup> transient peak was reduced by 37% in R25C-PLN cardiomyocytes and by 20% in WT-PLN cardiomyocytes, compared with the GFP group (Figure 4E and F), indicating a super-inhibitory effect of mutant-PLN on SR Ca<sup>2+</sup> content. However, the time constant for 50% decay of the caffeine-induced Ca<sup>2+</sup> transient ( $T_{50}$ ), which mainly reflects Ca<sup>2+</sup> extrusion by the sodium/calcium exchanger (NCX), was similar between the three groups (Figure 4G).

### 3.6 Isoproterenol stimulation relieves the inhibitory effects of R25C-PLN

Phospholamban has been postulated to be phosphorylated during  $\beta$ -adrenergic stimulation, resulting in relief of its inhibitory effects on SERCA2a and cardiac function.<sup>7</sup> To determine whether the super-

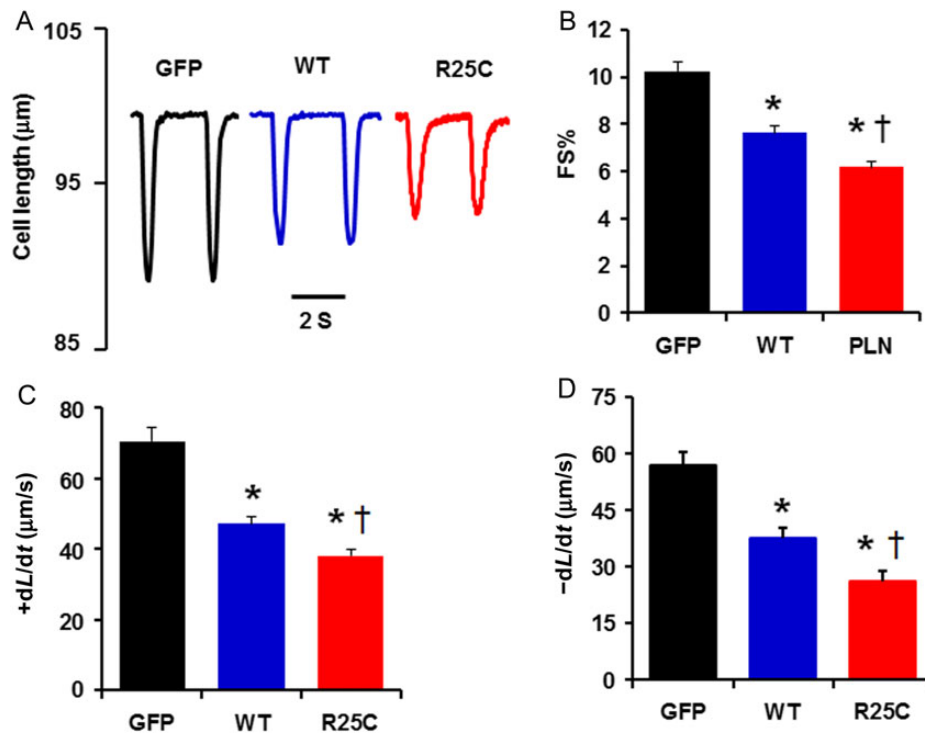


**Figure 3** Contractile parameters in Ad.GFP, Ad.WT-PLN, and Ad.R25C-PLN infected cardiomyocytes. (A) Representative cell-shortening traces of Ad.GFP, Ad.WT-PLN, and Ad.R25C-PLN cardiomyocytes (cell-length trace represents the percentage of resting cell length); (B) Fractional shortening (FS%); (C) Maximum rates of contraction (+dL/dt); (D) Maximum rates of relengthening (-dL/dt) (20–25 cells were measured per experiment or each heart;  $n = 4$  hearts for GFP, WT-PLN, and R25C-PLN groups). \* $P < 0.05$ , vs. GFP; † $P < 0.05$ , vs. WT. Values are mean  $\pm$  SE.

inhibitory effects of mutant PLN could be also relieved by  $\beta$ -agonists, cardiac myocytes infected with Ad.GFP, Ad.WT-PLN, or Ad.R25C-PLN were stimulated with isoproterenol and their mechanical and  $\text{Ca}^{2+}$  kinetic parameters were assessed. It is interesting to note that maximal stimulation, obtained at 100 nmol isoproterenol, resulted in complete reversal of the inhibitory effects of wild-type or mutant PLN. Similarly, under maximal isoproterenol stimulation, the inhibition on the amplitude of systolic  $\text{Ca}^{2+}$  transient and the rate of decay of this signal were fully reversed in cardiomyocytes overexpressing mutant PLN. The maximally stimulated values were similar among the three groups (see Supplementary material online, Figure S1).

### 3.7 The mutant R25C-PLN exhibits enhanced association to SERCA2 and PKA abrogates this effect

To gain insights into the mechanisms associated with increased inhibition of SERCA2a by R25C-PLN, we co-expressed SERCA2 with either WT or mutant PLN in HEK cells to evaluate their interactions in the absence of endogenous proteins. For this, we generated a GFP-WT-PLN or GFP-R25C-PLN constructs and transiently co-transfected these along with SERCA2 in HEK 293 cells. Initial immunofluorescence studies indicated that, similar to GFP-WT-PLN, the GFP-R25C-PLN mutant exhibited co-localization with SERCA2 in ER (Figure 5A). Subsequent immunoprecipitation studies from co-transfected cells revealed a significant increase in the levels of SERCA2 in the R25C-PLN sample, compared with WT-PLN (Figure 5B and C), indicating enhanced formation

of the SERCA2/R25C-PLN protein complex. Interestingly, parallel experiments in cell lysates, that had been previously phosphorylated by PKA, revealed that phosphorylation of R25C-PLN abolishes the increased interaction of this mutant with SERCA2, as similar levels of SERCA2 were observed in the phosphorylated R25C-PLN and WT-PLN protein complexes (Figure 5D and E). These findings are consistent with relief of the mutant PLN super-inhibitory effects on contractility and  $\text{Ca}^{2+}$ -cycling upon Iso-stimulation of cardiomyocytes (see Supplementary material online, Figure S1).

### 3.8 Increased $\text{Ca}^{2+}$ sparks, waves, diastolic SR $\text{Ca}^{2+}$ leak, and stress-induced aftercontractions in R25C-PLN cardiomyocytes

As described earlier, all R25C affected members in the family pedigree developed cardiac arrhythmias (Figure 1 and Table 1). The molecular trigger for arrhythmia is enhanced SR  $\text{Ca}^{2+}$  leak, evidenced by increases in  $\text{Ca}^{2+}$  sparks or waves at the cardiomyocyte level.<sup>23</sup> To determine the effect of R25C on SR  $\text{Ca}^{2+}$  release, we examined  $\text{Ca}^{2+}$  spark properties in intact quiescent cells. The line-scan and three-dimensional images for  $\text{Ca}^{2+}$  sparks are presented in Figure 6A. It was observed that spark frequency was two-fold in the mutant PLN cardiomyocytes, compared with WT-PLN or GFP cardiomyocytes (Figure 6B). Next, the frequency of spontaneous  $\text{Ca}^{2+}$  waves was examined in GFP, WT-PLN, and R25C-PLN myocytes. It was found that  $\text{Ca}^{2+}$  waves were developed in 40% of R25C cardiomyocytes, compared with 4% of WT-PLN cells

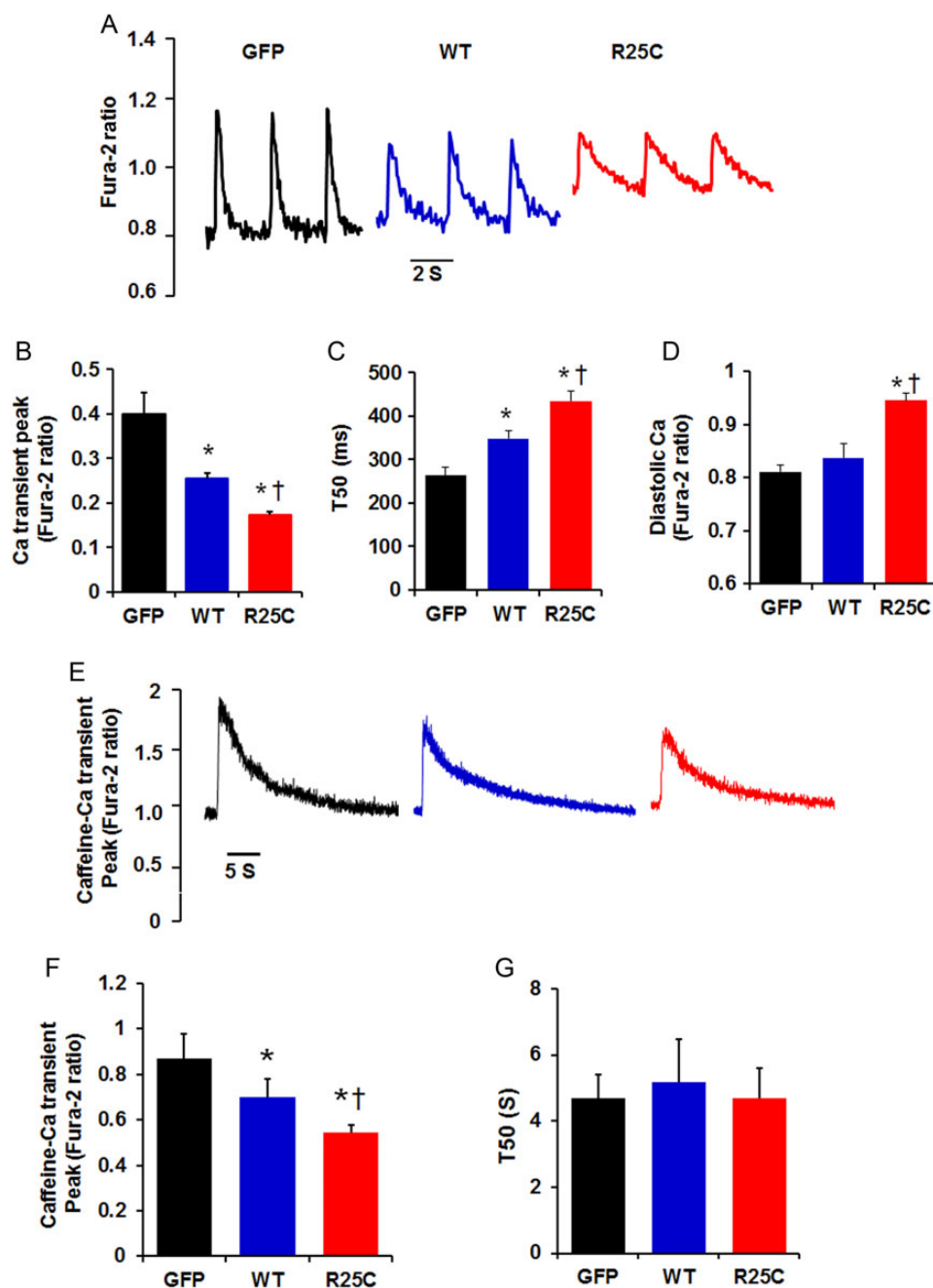


**Figure 4**  $\text{Ca}^{2+}$  kinetics in Ad.GFP, Ad.WT-PLN, and Ad.R25C-PLN cardiomyocytes. Infected myocytes were incubated with Fura-2/AM for half an hour and  $\text{Ca}^{2+}$  transients were measured. (A) Representative tracings of  $\text{Ca}^{2+}$  transients; (B)  $\text{Ca}^{2+}$  transient amplitude in infected cardiomyocytes; (C) Time to 50% decay (T50) of  $\text{Ca}^{2+}$  signal; (D) Intracellular diastolic  $\text{Ca}^{2+}$ ; (E) Representative tracings of caffeine (10 mM)-induced  $\text{Ca}^{2+}$  transient; (F) Caffeine-induced  $\text{Ca}^{2+}$  transient amplitude; (G) Time to 50% decay (T50) of caffeine-induced  $\text{Ca}^{2+}$  transient peak (20–25 cells were measured per experiment or each heart;  $n = 4$  hearts for GFP, WT-PLN, and R25C-PLN groups). \* $P < 0.05$ , vs. GFP; † $P < 0.05$ , vs. WT. Values are mean  $\pm$  SE.

and 6% of GFP cells (Figure 6C and D). Thus, R25C-PLN increases the frequency of  $\text{Ca}^{2+}$  sparks and  $\text{Ca}^{2+}$  waves in cardiomyocytes.

Recent studies have suggested that RyR2-mediated  $\text{Ca}^{2+}$  leak occurs in part as  $\text{Ca}^{2+}$  sparks, although there is RyR-mediated and  $\text{Ca}^{2+}$  spark-independent leak.<sup>24</sup> Therefore, total diastolic SR  $\text{Ca}^{2+}$  leak was also measured using the tertacaine protocol<sup>25</sup> (Figure 6E and F). The ratio of SR  $\text{Ca}^{2+}$  leak to SR  $\text{Ca}^{2+}$  load was significantly larger in R25C cardiomyocytes, compared with GFP and WT cardiomyocytes (Figure 6G), suggesting that R25C-PLN increases the SR  $\text{Ca}^{2+}$  leak.

Next, we determined the role of R25C-PLN under stress conditions by measuring the frequency of aftercontractions in GFP, WT-PLN, and R25C cardiomyocytes at 2-Hz field stimulation in the presence of 1  $\mu\text{M}$  Isoproterenol. Spontaneous aftercontractions occurred in 74% of R25C cells within 5 s after pacing was stopped, compared with 17% of WT-PLN and 16% of GFP cells (Figure 6H and I). Taken together, these findings suggest that overexpression of R25C-PLN enhances the propensity for spontaneous  $\text{Ca}^{2+}$  release from the SR, resulting in increased susceptibility to arrhythmia.

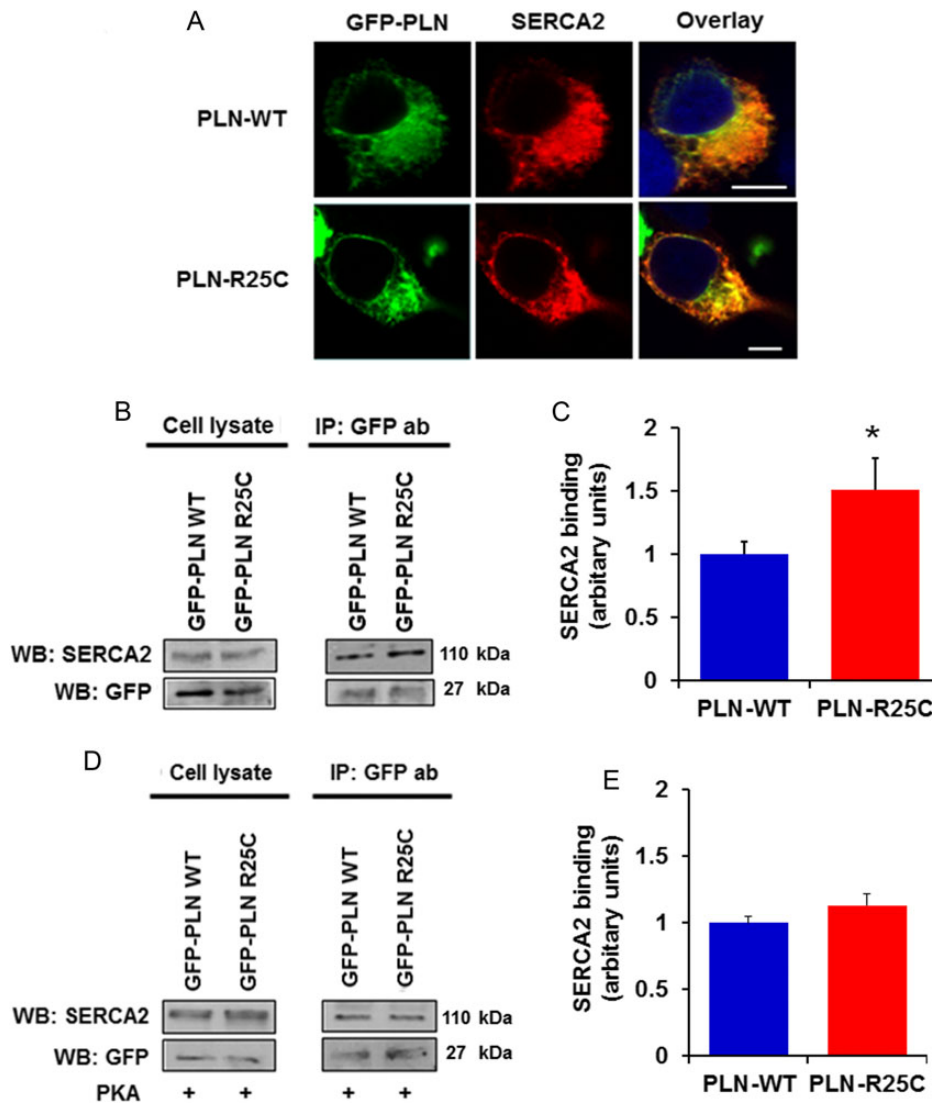


**Figure 5** (A) The R25C-PLN mutant co-localizes with SERCA2 in transfected HEK 293 cells, similar to WT-PLN. Nuclei are stained with DAPI. Scale bar, 5  $\mu\text{m}$ ; (B and C) R25C-PLN mutant exhibits enhanced association to SERCA2. Immunoprecipitation assays in HEK 293 cells that co-express GFP-PLN and SERCA2 were performed using GFP antibody. Quantification of SERCA2 levels revealed a significant increase in the SERCA2/R25C-PLN protein complex compared with GFP-WT-PLN ( $n = 4$ ) values are means  $\pm$  SE; \* $P < 0.05$ , compared with WT-PLN); (D and E) enhanced binding of R25C-PLN with SERCA2a was abolished upon PKA phosphorylation. Immunoprecipitations were performed in lysates from HEK 293 transfected cells that had been previously phosphorylated with PKA. Western blot analysis (D) determined similar levels of SERCA2 in both WT-PLN and R25C-PLN samples and quantitative analysis (E) showed no difference in SERCA2 binding between WT-PLN and R25C-PLN ( $n = 4$ ).

### 3.9 Increased SR $\text{Ca}^{2+}$ leak and arrhythmias in R25C myocytes are associated with augmented phosphorylation of RyR2 at serine-2814

We then investigated whether the increased SR  $\text{Ca}^{2+}$  leak in R25C cardiomyocytes was associated with increase in the phosphorylation of RyR2. Previous studies have shown that enhanced phosphorylation of Ser2808 (PKA site) and Ser2814 (CaMKII site) in RyR2 can regulate RyR2 function.<sup>26,27</sup> Thus, we examined the phosphorylation state of RyR2 in R25C cardiomyocytes, by performing western blots with phospho-specific antibodies against the RyR2 Ser2808 and Ser2814 sites. It was observed that R25C cells had significantly increased phosphorylation levels of RyR at Ser2814, but not at Ser2808

(Figure 7A–C). This prompted us to determine the activity of CaMKII in cell lysates from GFP, WT-PLN, and R25C cardiomyocytes, using a non-radiographic CaMKII ELISA. We found that the activity of CaMKII in R25C myocytes was increased to two-fold compared with WT-PLN or GFP groups (Figure 7D), consistent with the increase in diastolic  $\text{Ca}^{2+}$  in these cells (Figure 4D). To further confirm this finding, phosphorylation of CaMKII at Thr286 residue, which represents permanent activation of the CaMKII enzyme, was determined in cell lysates from GFP, WT-PLN, and R25C cardiomyocytes using western blots. It was observed that the level of phosphorylation of CaMKII at Thr286 was considerably higher in R25C cells, compared with the WT-PLN or GFP groups (Figure 7E and F). Interestingly, the increased CaM kinase activity did not reflect altered phosphorylation of PLN (see Supplementary material online, Figure S2) in the mutant cells,

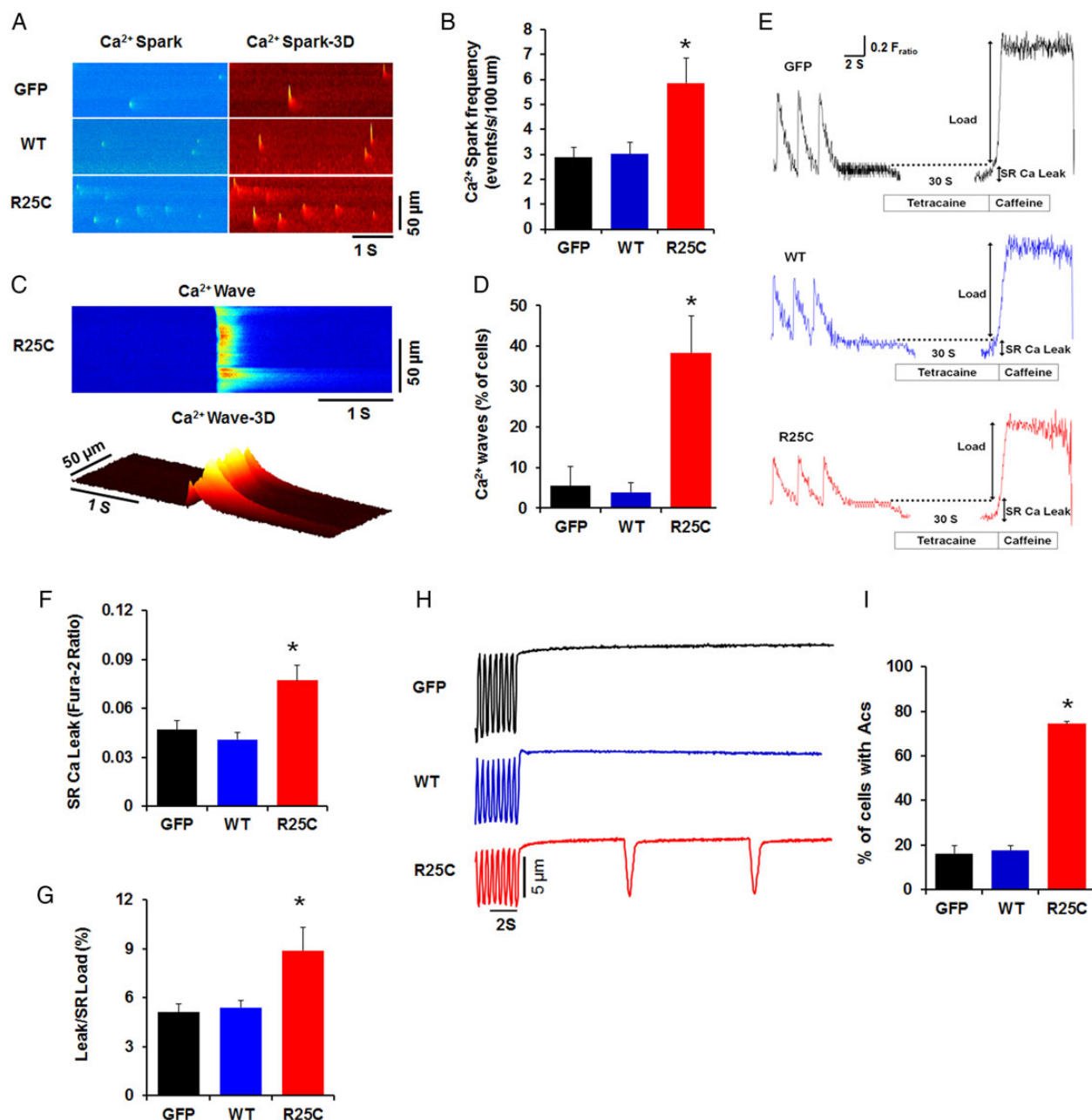


**Figure 6** Ca<sup>2+</sup> sparks, waves, diastolic SR Ca<sup>2+</sup> leak, and stress-induced aftercontractions (Acs) in GFP, WT-PLN, and R25C-PLN cardiomyocytes. (A) Representative line-scan and three-dimensional (3D) images of Ca<sup>2+</sup> sparks acquired in infected cardiomyocytes; (B) Cumulative data on Ca<sup>2+</sup> spark frequency; (C) Representative line-scan and 3D images of Ca<sup>2+</sup> waves acquired in R25C-PLN cardiomyocytes; (D) Percentage of cells showing Ca<sup>2+</sup> waves (10–15 cells were measured per experiment or each heart;  $n = 6$  hearts for GFP, WT-PLN, and R25C-PLN groups); (E) Representative traces of SR Ca<sup>2+</sup> leak were obtained from the three groups. Ca<sup>2+</sup> leak was determined as the tetracaine sensitive drop in diastolic  $-2$  ratio; (F) Comparison of average diastolic SR Ca<sup>2+</sup> leak; (G) Quantification of leak/SR load relationships in GFP, WT, and R25C myocytes (ratio of twitch Ca<sup>2+</sup> transient/caffeine-induced Ca<sup>2+</sup> transient (10–12 cells were measured per experiment or each heart;  $n = 4$  hearts for GFP, WT-PLN and R25C-PLN groups); \* $P < 0.05$ , vs. WT and GFP. Values are mean  $\pm$  SE. (H) Representative traces of Acs; (I) Percentage of the infected cardiomyocytes that developed Acs (10–12 cells were measured per experiment or each heart;  $n = 6$  hearts for GFP, WT-PLN, and R25C-PLN groups). \* $P < 0.05$ , vs. GFP and WT. Values are mean  $\pm$  SE.

suggesting that mutant PLN either altered CaMKII binding or increased PLN-phosphatase activity. To further examine the contribution of CaMKII mediated phosphorylation of RyR2 in the R25C-induced increases of Ca<sup>2+</sup> sparks and waves, KN93, the selective inhibitor of CaMKII was utilized in parallel studies with KN92 as a control. We

found that KN93 completely abrogated the increased Ca<sup>2+</sup> spark frequency (Figure 7G), indicating that the aberrant SR Ca<sup>2+</sup> release was contributed by the increased CaMKII phosphorylation of RyR. Furthermore, KN93 fully abolished the Ca<sup>2+</sup> waves, elicited by R25C-PLN (Figure 7H). These data suggest that the aberrant SR Ca<sup>2+</sup> leak and resultant



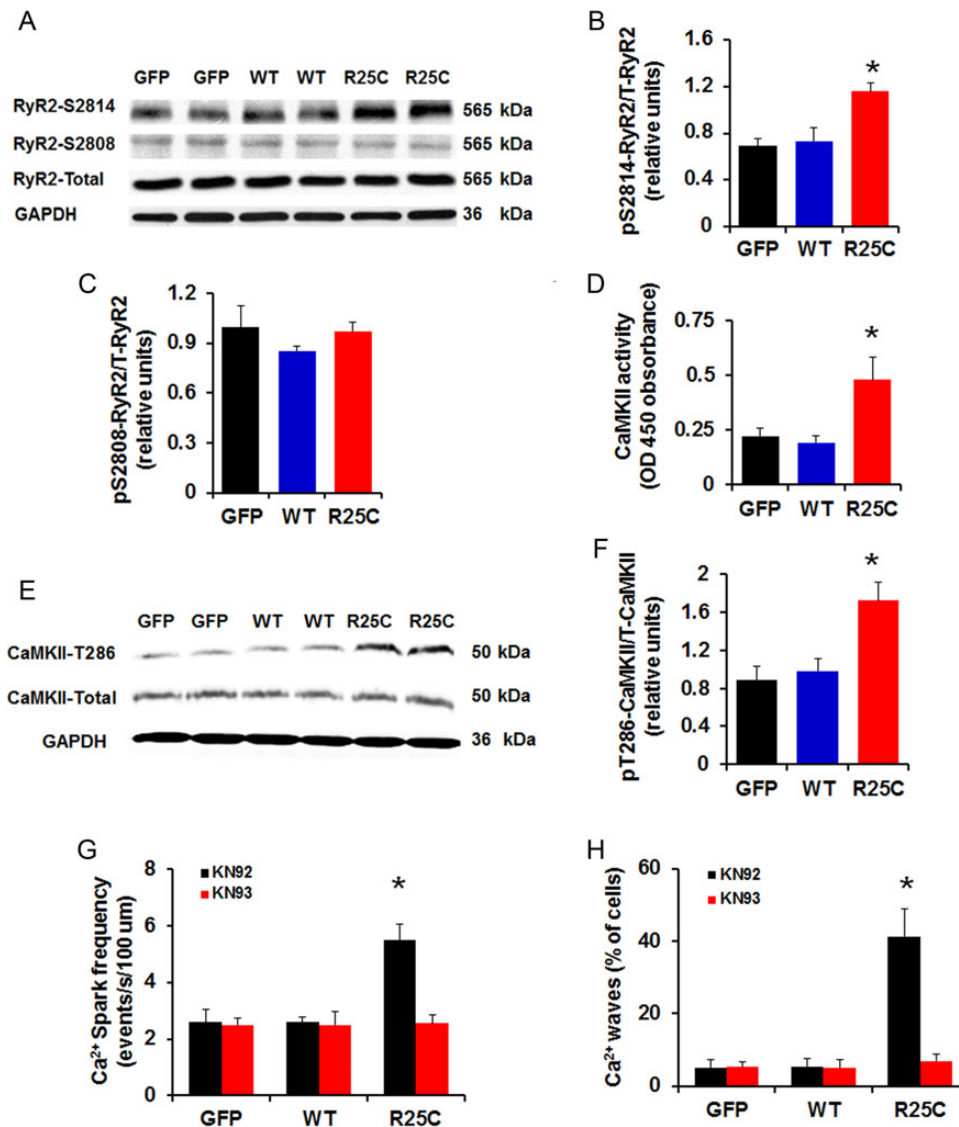


**Figure 7** Phosphorylation of RyR2 and CaMKII activity. (A) Representative blots of phosphorylation and total levels of RyR2; (B and C) Percentage of phosphorylated Ser2808 (pSer2808) and Ser2814 (pSer2814) RyR2 in infected cardiomyocytes ( $n = 6$  hearts); (D) CaMKII activity in GFP, WT, and R25C cardiomyocytes ( $n = 7$  hearts); (E) Representative blots of phosphorylation and total levels of CaMKII; (F) Percentage of phosphorylated Thr286 (pT286) CaMKII in infected cardiomyocytes ( $n = 4$  hearts); (G and H) Ca<sup>2+</sup> spark frequency and percentage of Ca<sup>2+</sup> waves recorded in GFP, WT, and R25C cardiomyocytes in the absence or presence of CaMKII inhibitor KN93 (1  $\mu\text{mol/L}$ ), with KN92 (1  $\mu\text{mol/L}$ ) used as a control (15–20 cells were measured per experiment or each heart;  $n = 4$  hearts for GFP, WT-PLN, and R25C-PLN groups). \* $P < 0.05$ , vs. WT-Basal, <sup>†</sup> $P < 0.05$ , vs. R25C-Basal. Values are mean  $\pm$  SE.

arrhythmia were associated with increased CaMKII activity and hyper-phosphorylation of RyR at Ser2814.

## 4. Discussion

In the current study, we identified a novel R25C-PLN mutation in familial DCM, which acts as a super-inhibitor of SERCA2a and results in decreased SR Ca<sup>2+</sup> content, Ca<sup>2+</sup> transients, and impaired contractile function. The depressed SR Ca<sup>2+</sup> resequestration is associated with increased CaMKII activity and hyper-phosphorylation of RyR2 at Ser2814, leading to aberrant Ca<sup>2+</sup>-leak and after-contractions under stress conditions. This is the first evidence that an experiment by

nature to alter PLN function results in increased SR Ca<sup>2+</sup>-leak and propensity to arrhythmia, a significant component of the cardiovascular phenotype observed in the carriers of the PLN mutation.

Our findings provide valuable new insights into the established paradigm of DCM gene/phenotype relationships. We<sup>1,28</sup> and others have suggested that the vast majority of DCM cases and families, shown to have genetic cause, appear monophenotypic—a classic ‘pure’ DCM with no atypical cardiovascular or syndromic features. For these families, ventricular or supraventricular arrhythmias have been attributed to a generic progression towards advanced heart failure with its manifold cellular abnormalities, including increased susceptibility to arrhythmia rather than a gene-specific abnormality. Dissecting between the

DCM-elicited arrhythmias and those resulting from a specific molecular defect remains challenging, although the exception has been the category of 'DCM with prominent arrhythmia',<sup>28</sup> assigned predominantly to variants in *LMNA*, but also observed with variants in *SCN5A*<sup>29</sup> or *DES*.<sup>30</sup> Our current work augments this established gene/phenotype paradigm, as previously reported rare variants in *PLN* have been associated with predominantly monophenotypic DCM, while the R25C *PLN* variant leads to prominent arrhythmias, which we suggest may be due in part to novel, specific mechanisms. These *PLN*-mutation carriers presented with arrhythmia in middle-age and in the setting of DCM, characterized by an 'adult-onset', as commonly observed in most of genetic cardiomyopathy. Another recent report with the R14del-*PLN* variant, a founder mutation in a large number of Dutch individuals, also suggested a propensity to arrhythmia, although a key predictor of arrhythmia was reduced systolic function (<45%).<sup>13</sup>

Previous studies regarding the role of super-inhibitor *PLN* mutants in mouse models suggested that the depressed *SERCA2* activity and contractility were associated with hypertrophic remodelling and ventricular failure over the long term.<sup>31,32</sup> Similar to those studies, our functional data further support the role of *PLN* mutations in DCM. The mechanisms underlying the super-inhibitory activity of R25C-*PLN* appear to include increased association or interaction of this mutant with *SERCA2a*, resulting in increased inhibition of SR  $\text{Ca}^{2+}$ -transport. Indeed, depressed SR  $\text{Ca}^{2+}$  cycling is a major characteristic of human and experimental heart failure. Accordingly, cardiac overexpression<sup>33</sup> or gene transfer<sup>34</sup> of *SERCA2a* in rat models of heart failure not only significantly improved cardiac contractile function, but increased survival and cardiac metabolism. Similarly, inhibition of *PLN* activity resulted in enhanced SR  $\text{Ca}^{2+}$  cycling and cardiac contractility<sup>34,35</sup> as well as attenuated heart-failure progression.<sup>36</sup> In addition, RyR inhibition by calstabin improved cardiac function in failing hearts.<sup>23</sup> These studies suggest that disturbed SR  $\text{Ca}^{2+}$  cycling may serve as a root cause of heart failure and this hypothesis has been well supported by recent studies in human patients.<sup>37,38</sup>

Interestingly, the R25C-*PLN* was also associated with increased  $\text{Ca}^{2+}$  sparks, waves, and stress-induced after-contractions, which may have contributed to the clinical features of cardiac arrhythmia in R25C carriers at the cellular level. The underlying pathways appear to involve increased inhibition of *SERCA2a* by mutant *PLN*, resulting in elevated diastolic  $\text{Ca}^{2+}$  and activation of CaMKII<sup>39</sup> (Figure 4D). Actually, several studies in neuron cells and cardiomyocytes have shown that sustained intracellular  $\text{Ca}^{2+}$  elevation enhances CaMKII auto-phosphorylation and increases  $\text{Ca}^{2+}$ /calmodulin-independent kinase activity.<sup>40–42</sup> The activation of CaMKII reflected enhanced phosphorylation of RyR2 at Ser2814, leading to increases in SR  $\text{Ca}^{2+}$  leak and arrhythmia, consistent with previous studies.<sup>42–44</sup> Indeed, inhibition of CaMKII activity by KN93 abrogated the increases in  $\text{Ca}^{2+}$ -sparks and  $\text{Ca}^{2+}$ -waves, elicited by R25C-*PLN*. Notably, overexpression of WT-*PLN* in cardiomyocytes, which resulted in a smaller degree of *SERCA2a* inhibition than R25C-*PLN*, did not significantly alter diastolic  $\text{Ca}^{2+}$  levels, CaMKII activity or phosphorylation of RyR2 at Ser2814. These findings indicate that inhibition of *SERCA2a* beyond a threshold point has detrimental effects through increased diastolic  $\text{Ca}^{2+}$  levels and CaMKII activation.

The mechanisms associated with the super-inhibitory effects of R25C-*PLN* are likely mediated through a disturbed conformational structure of *PLN*. Arg25 is highly conserved across species and this residue supplies a positive charge, which is important for maintaining the hinge region of *PLN* in the hydrophilic cytosolic environment. Thus, the Arg25 replacement with cysteine, a non-polar amino acid,

could destabilize the hinge angle, leading to conformational changes that enhance the association between *PLN* and *SERCA2a*.<sup>45</sup> Interestingly, the super-inhibitory effects of mutant *PLN* were completely relieved upon isoproterenol stimulation, which also reduced the binding of R25C-*PLN* with *SERCA2* to similar levels as WT-*PLN*, indicating that this mutation did not alter the ability of *PLN* to get phosphorylated. Future studies on the three-dimensional structure of mutant *PLB* and *SERCA2a* will provide insights into the mechanisms by which R25C-*PLN* exerts its inhibitory effects and may contribute to design of appropriate molecules to relieve *PLB* inhibition on *SERCA2a* and improve function in DCM carriers.

In summary, the current study demonstrates that a newly identified human R25C-*PLN* mutant is associated with DCM and increased propensity to arrhythmias. Our findings support the view that suppression of  $\text{Ca}^{2+}$ -resequestration by the SR may result in depressed contractility as well as activation of other detrimental pathways, which further exacerbate impaired  $\text{Ca}^{2+}$ -handling, resulting in arrhythmias and deteriorative remodelling. Thus, the mutation reported in this study, together with the previously reported human *PLN* mutations, point to the paramount importance of genetic and cardiac screening for these rare exome variants that disrupt normal homeostatic mechanisms for calcium cycling in the human heart.

## 5. Limitations

Other factors, including environmental or other genetic perturbations, may have also contributed to the R25C-*PLN* human phenotype. However, the clinical, pedigree, and functional data are compelling and congruent with prior reports of *PLN* mutations causing DCM.

## Supplementary material

Supplementary Material is available at *Cardiovascular Research* online.

## Acknowledgements

We thank the families and referring physicians for their participation in the Familial Dilated Cardiomyopathy Research Program.

**Conflict of interest:** none declared.

## Funding

This work was supported by the National Institutes of Health (HL26057 and HL64018 to E.G.K., HL58626 to R.E.H.); and the European Community's Seventh Framework Program (FP7/2007-2013 under grant agreement no. HEALTH-F2-2009-241526, EUTrigTreat to E.G.K.)

## References

- Hershberger RE, Hedges DJ, Morales A. Dilated cardiomyopathy: the complexity of a diverse genetic architecture. *Nat Rev Cardiol* 2013;**10**:531–547.
- Beuckelmann DJ, Nabauer M, Erdmann E. Intracellular calcium handling in isolated ventricular myocytes from patients with terminal heart failure. *Circulation* 1992;**85**:1046–1055.
- Gwathmey JK, Copelas L, MacKinnon R, Schoen FJ, Feldman MD, Grossman W, Morgan JP. Abnormal intracellular calcium handling in myocardium from patients with end-stage heart failure. *Circ Res* 1987;**61**:70–76.
- Hasenfuss G. Alterations of calcium-regulatory proteins in heart failure. *Cardiovasc Res* 1998;**37**:279–289.
- Meyer M, Schillinger W, Pieske B, Holubarsch C, Heilmann C, Posival H, Kuwajima G, Mikoshiba K, Just H, Hasenfuss G. Alterations of sarcoplasmic reticulum proteins in failing human dilated cardiomyopathy. *Circulation* 1995;**92**:778–784.
- MacLennan DH, Kranias EG. Phospholamban: a crucial regulator of cardiac contractility. *Nat Rev Mol Cell Biol* 2003;**4**:566–577.

7. Kranias EG, Hajjar RJ. Modulation of cardiac contractility by the phospholamban/SERCA2a regulome. *Circ Res* 2012;**110**:1646–1660.
8. Haghghi K, Schmidt AG, Hoit BD, Brittsan AG, Yatani A, Lester JW, Zhai J, Kimura Y, Dorn GW II, MacLennan DH, Kranias EG. Superinhibition of sarcoplasmic reticulum function by phospholamban induces cardiac contractile failure. *J Biol Chem* 2001;**276**:24145–24152.
9. Haghghi K, Kolokathis F, Pater L, Lynch RA, Asahi M, Gramolini AO, Fan GC, Tsiapras D, Hahn HS, Adamopoulos S, Liggett SB, Dorn GW II, MacLennan DH, Kremastinos DT, Kranias EG. Human phospholamban null results in lethal dilated cardiomyopathy revealing a critical difference between mouse and human. *J Clin Invest* 2003;**111**:869–876.
10. Schmitt JP, Kamisago M, Asahi M, Li GH, Ahmad F, Mende U, Kranias EG, MacLennan DH, Seidman JG, Seidman CE. Dilated cardiomyopathy and heart failure caused by a mutation in phospholamban. *Science* 2003;**299**:1410–1413.
11. Haghghi K, Kolokathis F, Gramolini AO, Waggoner JR, Pater L, Lynch RA, Fan GC, Tsiapras D, Parekh RR, Dorn GW II, MacLennan DH, Kremastinos DT, Kranias EG. A mutation in the human phospholamban gene, deleting arginine 14, results in lethal, hereditary cardiomyopathy. *Proc Natl Acad Sci USA* 2006;**103**:1388–1393.
12. Posch MG, Perrot A, Geier C, Boldt LH, Schmidt G, Lehmkuhl HB, Hetzer R, Dietz R, Gutberlet M, Haverkamp W, Ozcelik C. Genetic deletion of arginine 14 in phospholamban causes dilated cardiomyopathy with attenuated electrocardiographic R amplitudes. *Heart Rhythm* 2009;**6**:480–486.
13. van Rijsingen IA, van der Zwaag PA, Groeneweg JA, Nannenberg EA, Jongbloed JD, Zwinderman AH, Pinto YM, Lekanne Dit Deprez RH, Post JG, Tan HL, de Boer RA, Hauer RN, Christiaans I, van den Berg MP, van Tintelen JP, Wilde AA. Outcome in Phospholamban R14del Carriers: Results of a Large Multicentre Cohort Study. *Circ Cardiovasc Genet* 2014;**7**:455–465.
14. Cowan J, Li D, Gonzalez-Quintana J, Morales A, Hershberger RE. Morphological analysis of 13 LMNA variants identified in a cohort of 324 unrelated patients with idiopathic or familial dilated cardiomyopathy. *Circ Cardiovasc Genet* 2010;**3**:6–14.
15. Parks SB, Kushner JD, Nauman D, Burgess D, Ludwigsen S, Peterson A, Li D, Jakobs P, Litt M, Porter CB, Rahko PS, Hershberger RE. Lamin A/C mutation analysis in a cohort of 324 unrelated patients with idiopathic or familial dilated cardiomyopathy. *Am Heart J* 2008;**156**:161–169.
16. Norton N, Li D, Rampersaud E, Morales A, Martin ER, Zuchner S, Guo S, Gonzalez M, Hedges DJ, Robertson PD, Krumm N, Nickerson DA, Hershberger RE. Exome sequencing and genome-wide linkage analysis in 17 families illustrate the complex contribution of TTN truncating variants to dilated cardiomyopathy. *Circ Cardiovasc Genet* 2013;**6**:144–153.
17. Hu ST, Shen YF, Liu GS, Lei CH, Tang Y, Wang JF, Yang YJ. Altered intracellular Ca<sup>2+</sup> regulation in chronic rat heart failure. *J Physiol Sci* 2010;**60**:85–94.
18. Luo W, Grupp IL, Harrer J, Ponniah S, Grupp G, Duffy JJ, Doetschman T, Kranias EG. Targeted ablation of the phospholamban gene is associated with markedly enhanced myocardial contractility and loss of beta-agonist stimulation. *Circ Res* 1994;**75**:401–409.
19. Arvanitis DA, Vafiadaki E, Fan GC, Mitton BA, Gregory KN, Del Monte F, Kontogianni-Konstantopoulos A, Sanoudou D, Kranias EG. Histidine-rich Ca-binding protein interacts with sarcoplasmic reticulum Ca-ATPase. *Am J Physiol Heart Circ Physiol* 2007;**293**:H1581–H1589.
20. Knollmann BC, Chopra N, Hlaing T, Akin B, Yang T, Etensohn K, Knollmann BE, Horton KD, Weissman NJ, Holinstat I, Zhang W, Roden DM, Jones LR, Franzini-Armstrong C, Pfeifer K. Casq2 deletion causes sarcoplasmic reticulum volume increase, premature Ca<sup>2+</sup> release, and catecholaminergic polymorphic ventricular tachycardia. *J Clin Invest* 2006;**116**:2510–2520.
21. Herman DS, Lam L, Taylor MR, Wang L, Teekakirikul P, Christodoulou D, Conner L, DePalma SR, McDonough B, Sparks E, Teodorescu DL, Cirino AL, Banner NR, Pennell DJ, Graw S, Merlo M, Di Lenarda A, Sinagra G, Bos JM, Ackerman MJ, Mitchell RN, Murry CE, Lakdawala NK, Ho CY, Barton PJ, Cook SA, Mestroni L, Seidman JG, Seidman CE. Truncations of titin causing dilated cardiomyopathy. *N Engl J Med* 2012;**366**:619–628.
22. Kadambi VJ, Ponniah S, Harrer JM, Hoit BD, Dorn GW II, Walsh RA, Kranias EG. Cardiac-specific overexpression of phospholamban alters calcium kinetics and resultant cardiomyocyte mechanics in transgenic mice. *J Clin Invest* 1996;**97**:533–539.
23. Wehrens XH, Lehnart SE, Reiken S, van der Nagel R, Morales R, Sun J, Cheng Z, Deng SX, de Windt LJ, Landry DW, Marks AR. Enhancing calstabin binding to ryanodine receptors improves cardiac and skeletal muscle function in heart failure. *Proc Natl Acad Sci USA* 2005;**102**:9607–9612.
24. Zima AV, Bovo E, Bers DM, Blatter LA. Ca(2)+ spark-dependent and -independent sarcoplasmic reticulum Ca(2)+ leak in normal and failing rabbit ventricular myocytes. *J Physiol* 2010;**588**:4743–4757.
25. Shannon TR, Pogwizd SM, Bers DM. Elevated sarcoplasmic reticulum Ca<sup>2+</sup> leak in intact ventricular myocytes from rabbits in heart failure. *Circ Res* 2003;**93**:592–594.
26. Shan J, Betzenhauser MJ, Kushnir A, Reiken S, Meli AC, Wronska A, Dura M, Chen BX, Marks AR. Role of chronic ryanodine receptor phosphorylation in heart failure and beta-adrenergic receptor blockade in mice. *J Clin Invest* 2010;**120**:4375–4387.
27. van Oort RJ, McCauley MD, Dixit SS, Pereira L, Yang Y, Respress JL, Wang Q, De Almeida AC, Skapura DG, Anderson ME, Bers DM, Wehrens XH. Ryanodine receptor phosphorylation by calcium/calmodulin-dependent protein kinase II promotes life-threatening ventricular arrhythmias in mice with heart failure. *Circulation* 2010;**122**:2669–2679.
28. Hershberger RE, Siegfried JD. Update 2011: clinical and genetic issues in familial dilated cardiomyopathy. *J Am Coll Cardiol* 2011;**57**:1641–1649.
29. McNair WP, Sinagra G, Taylor MR, Di Lenarda A, Ferguson DA, Salcedo EE, Slavov D, Zhu X, Caldwell JH, Mestroni L. SCN5A mutations associate with arrhythmic dilated cardiomyopathy and commonly localize to the voltage-sensing mechanism. *J Am Coll Cardiol* 2011;**57**:2160–2168.
30. van Spaendonck-Zwarts KY, van Hessem L, Jongbloed JD, de Walle HE, Capetanaki Y, van der Kooij AJ, van Langen IM, van den Berg MP, van Tintelen JP. Desmin-related myopathy. *Clin Genet* 2011;**80**:354–366.
31. Zvaritch E, Backx PH, Jirik F, Kimura Y, de Leon S, Schmidt AG, Hoit BD, Lester JW, Kranias EG, MacLennan DH. The transgenic expression of highly inhibitory monomeric forms of phospholamban in mouse heart impairs cardiac contractility. *J Biol Chem* 2000;**275**:14985–14991.
32. Zhai J, Schmidt AG, Hoit BD, Kimura Y, MacLennan DH, Kranias EG. Cardiac-specific overexpression of a superinhibitory pentameric phospholamban mutant enhances inhibition of cardiac function in vivo. *J Biol Chem* 2000;**275**:10538–10544.
33. Muller OJ, Lange M, Rattunde H, Lorenzen HP, Muller M, Frey N, Bittner C, Simonides W, Katus HA, Franz WM. Transgenic rat hearts overexpressing SERCA2a show improved contractility under baseline conditions and pressure overload. *Cardiovasc Res* 2003;**59**:380–389.
34. del Monte F, Williams E, Lebeche D, Schmidt U, Rosenzweig A, Gwathmey JK, Lewandowski ED, Hajjar RJ. Improvement in survival and cardiac metabolism after gene transfer of sarcoplasmic reticulum Ca(2+)-ATPase in a rat model of heart failure. *Circulation* 2001;**104**:1424–1429.
35. del Monte F, Harding SE, Dec GW, Gwathmey JK, Hajjar RJ. Targeting phospholamban by gene transfer in human heart failure. *Circulation* 2002;**105**:904–907.
36. Hoshijima M, Ikeda Y, Iwanaga Y, Minamisawa S, Date MO, Gu Y, Iwatate M, Li M, Wang L, Wilson JM, Wang Y, Ross Jr J, Chien KR. Chronic suppression of heart-failure progression by a pseudophosphorylated mutant of phospholamban via in vivo cardiac rAAV gene delivery. *Nat Med* 2002;**8**:864–871.
37. Jaski BE, Jessup ML, Mancini DM, Cappola TP, Pauly DF, Greenberg B, Borow K, Dittrich H, Zsebo KM, Hajjar RJ. Calcium upregulation by percutaneous administration of gene therapy in cardiac disease (CUPID Trial), a first-in-human phase 1/2 clinical trial. *J Card Fail* 2009;**15**:171–181.
38. Zsebo K, Yaroshinsky A, Rudy JJ, Wagner K, Greenberg B, Jessup M, Hajjar RJ. Long-term effects of AAV1/SERCA2a gene transfer in patients with severe heart failure: analysis of recurrent cardiovascular events and mortality. *Circ Res* 2014;**114**:101–108.
39. Zhang T, Brown JH. Role of Ca<sup>2+</sup>/calmodulin-dependent protein kinase II in cardiac hypertrophy and heart failure. *Cardiovasc Res* 2004;**63**:476–486.
40. Wehrens XH, Lehnart SE, Reiken SR, Marks AR. Ca<sup>2+</sup>/calmodulin-dependent protein kinase II phosphorylation regulates the cardiac ryanodine receptor. *Circ Res* 2004;**94**:e61–e70.
41. Eshete F, Fields RD. Spike frequency decoding and autonomous activation of Ca<sup>2+</sup>-calmodulin-dependent protein kinase II in dorsal root ganglion neurons. *J Neurosci* 2001;**21**:6694–6705.
42. Anderson ME, Braun AP, Wu Y, Lu T, Wu Y, Schulman H, Sung RJ. KN-93, an inhibitor of multifunctional Ca<sup>2+</sup>/calmodulin-dependent protein kinase, decreases early afterdepolarizations in rabbit heart. *J Pharmacol Exp Ther* 1998;**287**:996–1006.
43. Curran J, Tang L, Roof SR, Velmurugan S, Millard A, Shonts S, Wang H, Santiago D, Ahmad U, Perryman M, Bers DM, Mohler PJ, Ziolo MT, Shannon TR. Nitric oxide-dependent activation of CaMKII increases diastolic sarcoplasmic reticulum calcium release in cardiac myocytes in response to adrenergic stimulation. *PLoS One* 2014;**9**:e87495.
44. Erickson JR, Pereira L, Wang L, Han G, Ferguson A, Dao K, Copeland RJ, Despa F, Hart GW, Ripplinger CM, Bers DM. Diabetic hyperglycaemia activates CaMKII and arrhythmias by O-linked glycosylation. *Nature* 2013;**502**:372–376.
45. Kimura Y, Kurzydowski K, Tada M, MacLennan DH. Phospholamban regulates the Ca<sup>2+</sup>-ATPase through intramembrane interactions. *J Biol Chem* 1996;**271**:21726–21731.